Journal of Applied Polymer Science

Fabrication of quaternary composite scaffold from silk fibroin, chitosan, gelatin, and alginate for skin regeneration

Chhavi Sharma,[1] Amit K. Dinda,[2] Pravin D. Potdar,[3] Narayan C. Mishra[1]

[1]Department of Polymer and Process Engineering, Indian Institute of Technology Roorkee, Roorkee 247001, India
[2]Department of Pathology, All India Institute of Medical Sciences, New Delhi 110029, India
[3]Department of Molecular Medicine and Biology, Jaslok Hospital and Research Centre, Mumbai 400 026, India
Correspondence to: N. C. Mishra (E-mail: mishrawise@gmail.com)

ABSTRACT: Quaternary composite scaffold consisting of chitosan, alginate, gelatin, and silk fibroin, was fabricated by applying foaming method, for tissue engineering applications. The fabricated scaffold was evaluated for its applicability in skin tissue regeneration. The environmental scanning electron microscopy (ESEM) showed the presence of interconnected pores, mostly spread over the entire surface of the scaffold with mean pore size 92±11.8 μm and the porosity 88%. The scaffold showed good mechanical stability under physiological conditions as determined by short term mechanical stability testing. *In vitro* scaffold-degradation study showed no degradation at day 1 and from day 3 scaffold starts degrading. The degradation of the composite scaffold after 28 days was 38%. Less degradation rate of the scaffold might be beneficial, as it can provide sufficient time for the formation of neo-tissue and extracellular matrix (ECM) during tissue regeneration. *In vitro* cell culture studies by seeding L929 mouse fibroblast cells over composite scaffold showed good cell viability, proliferation, and adhesion as indicated by 3-(4,5-dimethylthiazol-2-yl-2,5-diphenyltetrazolium bromide) (MTT) assay and ESEM of cell-scaffold construct. Giemsa staining of L929 fibroblast cells over the scaffold showed fibroblastic morphology of L929 cells, having elongated cells with nuclei and faint cytoplasm, and these cells are positive for Oil Red stain and negative for Alizarin Red staining—indicating that they maintained their dermal fibroblastic phenotype and were not differentiated into any other cell types in presence of composite scaffold. Results of histological staining supports growth and viability of L929 fibroblasts over scaffold, thereby proving the great prospective of this scaffold for skin tissue engineering applications. © 2015 Wiley Periodicals, Inc. J. Appl. Polym. Sci. **2015**, *132*, 42743.

KEYWORDS: biocompatibility; biodegradable; biomaterials; biomimetic; composites

Received 1 April 2015; accepted 17 July 2015
DOI: 10.1002/app.42743

INTRODUCTION

Skin damage such as genetic disorders, acute trauma, chronic wounds, and surgical interventions is a major healthcare confront. Conventional means to treat the damaged skin, is skin grafting (autograft or allograft), but there are some limitations to skin grafting, which include donor site shortage, scarring, pain, and the risk of infection.[1] Therefore, nowadays scientists have been trying to apply tissue-engineering approach to prepare tissue-engineered skin grafts that will overcome the limitations associated with skin grafting.[2] Tissue engineering involves introduction of the cells onto the scaffold, allow the cells to adhere, and grow on to the scaffold and differentiate into a specific tissue, which can be implanted into the damaged area.

The tissue engineering scaffold should have some desired properties: it should be biocompatible, biodegradable, and must aid in cell adhesion, proliferation, and provide various cues to cells for differentiating into a specific tissue.[3–8] Besides these properties, the scaffold should be mechanically strong enough to support the cellular growth. Scaffold, if prepared from a single polymer, cannot impart all the required properties to the scaffold, whereas two or more polymers in combination, if used for scaffold fabrication, might generate a synergistic effect to provide good mechanical strength to the scaffold as well as facilitate cell adhesion, and proliferation.[3–6] And, that is why, nowadays, scientists have been focusing on fabricating scaffolds using multi-polymers (more than two polymers) to mimic the properties of ECM, which also consists of multi-polymers.[9] Here, in this study, we also focus on fabricating composite scaffold with multi-polymers, and more specifically with bio-polymers which are having good resemblance to natural ECM elements, especially in terms of biocompatibility and biodegradability.

Scaffold can be fabricated by various techniques, and there are some advantages as well as disadvantages associated with each

technique.[10] Among the available techniques, foaming method—generating polymer-foam upon agitation of polymer solution and thereby crosslinking the polymer-foam, is one of the simplest and most economic techniques available for scaffold fabrication.[6,11,12] Though foaming method is the simplest and cheapest one, but it was not given much attention for tissue engineering applications.

Here, we aim to fabricate a quaternary composite scaffold comprising of natural polymers, silk fibroin, chitosan, gelatin, and alginate, by applying foaming method, and to study its applicability in skin tissue engineering. The reason for choosing this polymer combination is discussed below.

Chitosan, being a widely used natural polymer in tissue engineering has structural similarities with glycosaminoglycans (GAGs—an important component of ECM).[13–15] Besides this, chitosan has antimicrobial and hemostatic properties.[16] Gelatin used here, is a hydrolyzed form of collagen and it is well known that the interactions of glycosaminoglycans with collagens and other glycoprotein in extracellular matrix play vital functions in cell adhesion and assemblage of extracellular matrix. Therefore, chitosan mixed with gelatin may provide different cues to the cells for tissue regeneration.

Alginate, a biopolymer, is known to provide mechanical strength to the scaffold and it also plays a significant role in transmitting preliminary mechanical signals to the cells and developing tissue.[17] Alginate, together with gelatin and silk, produce a huge quantity of highly stable foam, and without highly stable foam we cannot fabricate scaffold by applying foaming method.

One disadvantage of chitosan, alginate, and gelatin is that they do not have good mechanical properties for fabricating scaffold favoring tissue (e.g., skin) regeneration. The mechanical properties of these polymers can be enhanced to great extent by combining them with silk.[18] There have been reports on silk fibroin/chitosan blend membranes with good mechanical properties forming an interpenetrating polymer network.[19]

Silk, a unique family of proteins from silkworms and spiders, is basically composed of two proteins: hydrophobic fibroin and hydrophilic sericin. Silk fibroin is the structural protein of fibers that consists of 18 amino acids, glycine, alanine, sericine, etc. which can give different cues for tissue regeneration.[20,21] Silk fibroin with its good mechanical properties, oxygen, and water vapor permeability, biocompatibility, and biodegradability can be a good candidate for fabricating scaffold for tissue regeneration.[22,23]

In the light of the useful properties (as mentioned above) of silk fibroin, chitosan, gelatin, and alginate, we expect that if we fabricate a scaffold consisting of all these polymers, the synergistic effect of all these polymers might make the scaffold highly suitable for tissue regeneration. Here we have investigated the possibility of fabricating a silk fibroin–chitosan–gelatin–alginate quaternary composite scaffold by applying foaming method to make it highly compatible for tissue engineering, and evaluated the scaffold for skin tissue regeneration.

We believe that the combination of the four natural biopolymers, silk fibroin, chitosan, gelatin, and alginate, to fabricate tissue engineering scaffold by applying foaming method, is unique, and to the best of our knowledge, we are the first to fabricate such quaternary composite scaffold.

MATERIALS

Chitosan (MW 100,000–300,000; ACS grade), was obtained from Sigma, St. Louis, MO. Alginate (300 kDa; ACS grade) were purchased from Acros Organics, New Jersey. Sodium bicarbonate ($NaHCO_3$), calcium chloride, and glacial acetic acid were obtained from Qualigens Fine Chemicals, Mumbai, India. Gelatin (ACS grade) was obtained from Merck Specialities Pvt., Mumbai and glutaraldehyde was purchased from SD Fine-Chem. Sodium carbonate (Na_2CO_3) and Lithium bromide (LiBr) were purchase from Hi-media, Mumbai, India. 3-(4,5-Dimethylthiazol-2-yl-2,5-diphenyltetrazolium bromide) (MTT) and Dimethyl sulfoxide (DMSO) was purchased from Hi-media, Mumbai, India. Glycine and lysozyme were also purchased from Hi-media, Mumbai, India. Dulbecco's modified eagle medium (DMEM) and phosphate buffer saline (PBS) were obtained from Sigma, St. Louis, MO. Fetal bovine serum (FBS) was received from Hyclone, and L929 mouse skin fibroblast cell line was received from NCCS, Pune, India. Trypsin-Ethylenediaminetetraacetic acid (EDTA) solution was obtained from Sigma, St. Louis, MO. Silk fibroin protein was isolated from *Bombyx mori* silkworm fresh cocoons purchased from Central Sericulture Silk Farm, Dehradun, India. Giemsa, Alizarin Red stain, and Trizol were purchased from Fisher Scientific, Mumbai, India. Oil Red stain was purchased from Sigma St. Louis, MO. Double distilled water was prepared in our laboratory and the same was used for preparing the polymer solution as well as for washing the scaffold. The cell culture reagents used here are of ReagentPlus® Grade (Purity $\geq$ 98.5%) unless otherwise noted. FBS have impurity level of $\leq$10 EU/mL endotoxin. Lysozyme used here is of premium quality level. Alizarin, Giemsa, and Oil Red dye were of highest purity analytical reagent grade. All materials were used without any further purification.

METHODS

Fabrication of Composite Scaffold Using Silk Fibroin

Preparation of Aqueous Silk Fibroin Solution and Scaffold Fabrication. Aqueous silk fibroin solution was prepared following the protocol described in previous literature.[24] Firstly, pupas were removed from the *Bombyx mori* cocoon and then the dried cocoons were cut into small pieces, and treated with boiling aqueous solution of 0.02*M* sodium carbonate (Na_2CO_3) for 1 h under constant stirring. The whole mass was repeatedly washed with sterilized water to remove the glue-like sericin protein and dried in hot air oven at 50°C for 1 h. Silk fibroin solution was prepared by dissolving degummed silk in 9.3*M* LiBr solution at 70°C for $2^1/_2$ h, yielding a 20% (w/v) solution. The fibroin solution (50 mL) was dialyzed in a cellulose membrane based dialysis cassette (molecular cutoff 12,400) against sterilized water for three days, changing water every 6 h in order to remove LiBr [Figure 1(A)]. After dialysis, silk fibroin solution was centrifuged at 5–10°C and 9000 rpm for 20 min to remove undissolved particles. The concentrated solution was stored at 4°C for further use in scaffold fabrication. The final concentration of fibroin

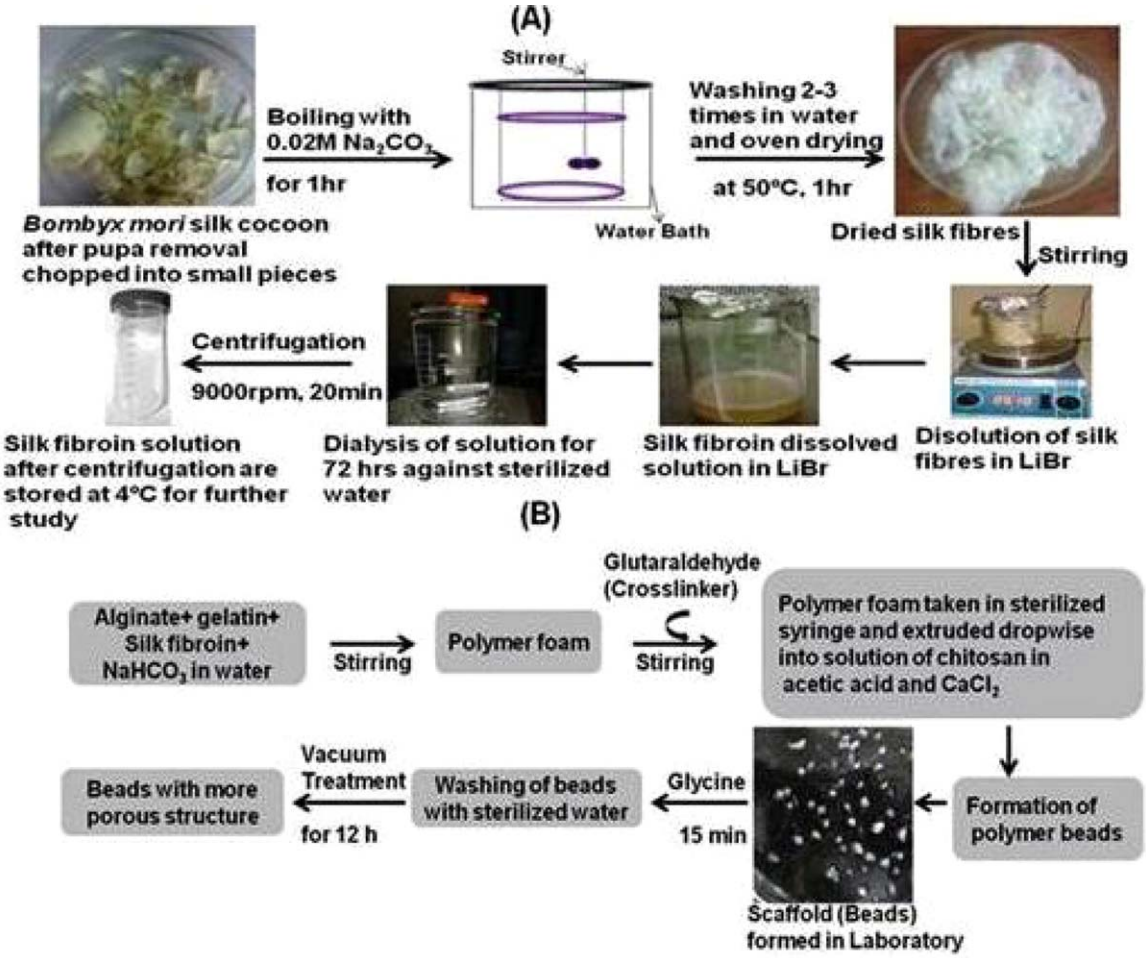

Figure 1. (A) Extraction of Silk Fibroin from *Bombyx mori* Cocoons; (B) Schematic showing foaming method of silk fibroin–chitosan–gelatin–alginate composite scaffold fabrication. [Color figure can be viewed in the online issue, which is available at wileyonlinelibrary.com.]

protein in aqueous solution was 1.6 mg/mL as determined by Lowry assay taking bovine serum albumin as standard.[25]

Scaffold Fabrication. The silk fibroin–chitosan–gelatin–alginate scaffold was fabricated by earlier used foaming method,[12] as described in Figure 1(B). Briefly, silk fibroin (containing 1.6 mg/mL fibroin protein) was mixed with alginate (2 wt %) and gelatin (5 wt %) in the volume ratio of 1 : 1 : 1. Thereafter, 0.9% sodium bicarbonate ($NaHCO_3$), a gas-generating agent, was added to this mixture, and was continuously stirred for 2 h. Next, 0.025% glutaraldehyde solution, crosslinker for chitosan, and gelatin was added to the alginate–gelatin–fibroin–$NaHCO_3$ mixture (volume ratio 1 : 50), and allowed to react/crosslink with the mixture for 10 h under continuous agitation. Because of the continuous agitation/stirring, foam was generated extensively. Scaffold in bead form, was formed by dropwise extrusion of the foam (alginate–gelatin–silk fibroin) into a solution containing chitosan in acetic acid and $CaCl_2$—a crosslinking agent for alginate [Figure 1(B)].[11,26] Here, the solution containing chitosan, acetic acid, and $CaCl_2$, was prepared by mixing a "solution of 2 wt % chitosan in 1 wt % acetic acid" with a "solution of 0.1*M* $CaCl_2$", in the volume ratio of 10 : 1. During the bead formation, acetic acid reacts with $NaHCO_3$ to evolve CO_2 from inside the bead, promoting high porosity in the bead-scaffold. The beads were allowed to remain in solution for 12 h, to facilitate efficient crosslinking among alginate, gelatin, and chitosan, and washed with sterilized water 20 times to remove excess glutaraldehyde. Scaffolds were then treated with glycine solution (1*M* for 15 min) in order to block any free aldehyde groups. After glycine treatment, scaffold beads were washed with sterilized water twice. Finally, the scaffold beads were exposed to vacuum for 12 h to create more porous structures inside. The fabricated scaffold was characterized and evaluated for skin tissue engineering applications.

SCAFFOLD CHARACTERIZATION

Scaffold Morphology

Morphology of composite scaffold was studied by using environmental scanning electron microscope (ESEM) (Quanta 200, FEI, The Netherlands). The scaffold in their hydrated form was observed directly, since the ESEM technique does not require dehydration of samples. To study the surface morphology of the scaffold, 15 composite beads were examined through ESEM at the saturation pressure of water vapor (1 torr) and an accelerating voltage of 15 KV. Each time five beads prepared from independent experiments were examined. Cross-section of the

scaffold was also examined after sectioning or cutting the other beads of same type with a sharp razor blade. The size of the pores was determined for the 30 beads by using image-J analysis software, and the average pore size was calculated.

Fourier Transform Infrared Spectroscopy (FT-IR)

Fourier transform infrared spectroscopy (FT-IR) is an important tool to carry out semi-quantitative functional analysis and to investigate intermolecular interaction between different compounds. In FT-IR, the wavelengths of many IR absorption bands is an indicative of definite type of chemical bonds while the shifts in band intensities and positions are caused by changes in the environment of the molecule, enabling description of variations in the environment. Infrared (IR) spectra were recorded with a Nexus Thermo FT-IR spectrophotometer (Nicolet Co.). The samples were prepared by processing compressed potassium bromide (KBr) disks. The ratio of sample to KBr used for performing FT-IR analysis was 1 mg sample/900 mg KBr.

Porosity

Porosity is defined as the percentage of void space in a solid and it is a morphological property independent of the material.[27] The porosity of composite beads was determined by liquid displacement method. In brief, beads were placed in a graduated cylinder filled with a known volume of ethanol (V_1). The total volume following bead immersion was recorded (V_2). The beads were removed with the volume V_T whereby, solvent is entrapped in the pores, and the remaining volume of ethanol in the graduated cylinder was denoted by (V_3). The total volume (V_T) of the beads was calculated according to eq. (1):

$$V_T = V_2 - V_3 \tag{1}$$

The porosity was determined using the following eq. (2):

$$\chi = \frac{V_1 - V_3}{V_T} \times 100 \tag{2}$$

The porosity-determination experiment was repeated six times, and the mean porosity was calculated.

Evaluation of Mechanical Stability

A short-term stability assay was carried out to study the behavior of the beads submitted to a combination of destabilizing forces so as to mimic the physiological conditions. The procedure was based on Orive *et al.* with some modifications.[28] Briefly, 10 beads were taken in a beaker containing 10 mL of PBS (pH=7.4) and the beaker was placed in a shaker at 200 rpm at room temperature. The beads from the beaker were examined under stereo microscope after 48 h. Results are expressed as the percentage of ruptured beads as a function of time and the stereo microscopy images showing ruptured beads after 48 h. The mechanical strength of the glycine treated collagen/chitosan microspheres was also determined in previous studies after 48 h of agitation by a similar method.[12]

Swelling Property

The swelling gives a measure of hydrophilicity and it is defined by the following equation:

$$S = ((w_s - w_d)/w_d) \times 100\% \tag{3}$$

where S = percentage swelling, w_s = wet weight of the bead-scaffold after swelling, and w_d = weight of the bead-scaffold after drying.

Briefly, the beaded scaffolds were immersed in phosphate buffer saline (PBS) (pH=7.4) at room temperature for an hour. After 1 h immersion, in every 10 min, a known quantity of the bead-scaffolds was retrieved and excess water was removed using filter paper. The wet weight of the scaffold (w_s) was determined using an electronic balance, after which the swollen scaffold was dried in an oven at 50°C for half an hour, and the dry weight (w_d) was measured. Each time, the percentage swelling (S) was calculated from the values of w_s and w_d. The experiment was carried out until the time point, where no further swelling of beads was observed and the equilibrium point of swelling of beads was determined. The experiment was repeated six times individually.

In Vitro Enzymatic Biodegradation

Degradability of the scaffold was determined by mass change of scaffold beads after their incubation in 1 mL PBS (pH 7.4) containing 1.6 μg/mL of lysozyme (100,000 U/mg).[29] A known quantity ($w_i = 0.5$ g) of freshly prepared beads were taken in a tissue culture plate in triplicate. To determine the degradation profile, the beads were removed from lysozyme solution in PBS after first, third, fifth, seventh, 14th, 21st, and 28th day and weighed (w_f). The extent of the *in vitro* degradation was calculated as the percentage of weight difference of the scaffold before and after hydrolysis with the lysozyme solution by the following equation:

$$\%\ \text{weight loss} = \frac{w_i - w_f}{w_i} \times 100 \tag{4}$$

The pH value of the resultant PBS solution was also measured using pH meter at different time intervals.

Cell Behavior on the Scaffold

Cell Viability, Proliferation, and Attachment Over the Scaffold. L929 cells were cultured as monolayers in DMEM media supplemented with 10% FBS, penicillin (100 units/mL), and streptomycin (100 μg/mL). Sub-confluent cultures of L929 fibroblasts from 50 mm culture flask were detached by trypsinization using 0.25% Trypsin–EDTA, resuspended in complete growth medium, and the cells counting was done by using a hemocytometer (Chemometec, Denmark).

For MTT and cell morphology study experiments, 5×10^3 cells of L929 cells were plated per well with and without scaffold in 96-well plates and fed with respective growth medium. The culture plates were incubated at 37°C in CO_2 incubator for 1, 3, and 5 days, respectively. After specific intervals, the cells were further processed for MTT and cell morphology analysis as mentioned below. The experiment was repeated six times individually.

In order to evaluate the cytotoxicity of the scaffold, a viability assay of composite scaffold was performed. This test is based on mitochondrial viability, as only functional mitochondria can oxidize the MTT solution, giving a typical blue–violet end product indicating the viability of cells.

L929 mouse fibroblast cells were used to check the compatibility of scaffold[30,31] for skin tissue engineering. Prior to cell seeding, the scaffolds were sterilized by exposing to UV light from a mercury arc lamp source under the laminar flow hood. Scaffolds were then placed in tissue culture plate and soaked with

100 μL DMEM overnight at 37°C in CO_2 incubator to make scaffold surface more efficient for cell attachment. Scaffolds were placed in 96-well tissue culture wells (1 bead/well) and incubated with L929 cells at three time points, e.g., 1, 3, and 5 days, at 37°C in CO_2 incubator to test the toxicity of leachable from the scaffold toward L929 fibroblast cells along with the control i.e. cells incubated in complete DMEM media without scaffold. After the incubation, the medium from these wells were removed and 90 μL of fresh complete growth media was added to the wells. Then 10 μL of MTT solution (5 mg/mL stock in PBS) was added to the media to make final volume of 100 μL. The plates were incubated at 37°C for 4 h until purple formazan crystals were formed due to reduction of MTT by viable cells. The media and beads were removed from the well and 200 μL of dimethyl sulfoxide (DMSO) was added to each well to dissolve the formazan crystals. Absorbance was taken on Bio-rad ELISA plate reader at 490 nm with the subtraction for plate absorbance at 620 nm. The absorbance (O.D.) is directly proportional to the amount of metabolically active cells i.e., cell viability. The results were expressed by comparing the absorbance values (O.D.) of cell-scaffold construct with the control values.

Morphology of the cells over the composite scaffold after cell culture was studied in their wet form using ESEM (Quanta 200, FEI, The Netherlands). For this purpose, L929 cells over the scaffolds were fixed with glutaraldehyde (2.5%) at 4°C for 6 h, then rinsed with PBS, and observed under ESEM.

Phase-contrast microscopy for the acquisition of cell images were carried out with cultured L929 fibroblasts on composite scaffold. After the incubation of cells with scaffold, the cell-scaffold constructs were viewed under an inverted phase-contrast microscope (Zeiss, India (Bangalore) Pvt.) and photographed.

Histology of L929 Cells on Scaffold. L929 cell cultures were set up in 48-well plates to study morphological features of these cells on to the scaffold. Histological staining of these cells was performed after incubation of 5×10^3 of L929 cells with scaffold for five days at 37°C in CO_2 incubator. The cell-scaffold constructs were subjected to three different stains to reveal their morphological phenotypes of skin as mentioned below. For each stain, six individual cell-scaffold constructs were examined under phase contrast microscope and photographed.

Alizarin Red staining. Alizarin Red is used in a biochemical assay to determine, the presence of calcific deposition by cells of an osteogenic lineage. As such, it is a marker of matrix mineralization, which is a decisive step towards the formation of calcified extracellular matrix associated with true bone.[32] Cells were cultured for five days with a composite scaffold. Alizarin red staining of cell-scaffold constructs was performed by fixing the cells over the scaffold with 70% chilled ethanol for 1 h at room temperature. The ethanol was then aspirated and the cell-scaffold construct was washed with distilled water thrice. Now alizarin red stain was added and allowed to incubate for 30 min at room temperature. The stain was aspirated. The cell-scaffold constructs were washed with distilled water 4–5 times and examined under phase contrast microscope and photographed.

Giemsa staining. The L929 fibroblast cells were cultured for five days with a composite scaffold. The cells on the scaffold were fixed with 50% methanol for 1 h at room temperature. Geimsa stain was added to it and the cell-scaffold construct was washed with distilled water after 5 min. The stained cells over the scaffold were observed under phase contrast microscope and photographed.

Oil Red staining. The L929 fibroblast cells were cultured for five days with a composite scaffold. The cells on the scaffold were fixed with 50% methanol for 1 h at room temperature. Now, 2 mL of 60% isopropanol was added to it for 5 min. After this, oil red stain was applied to the cell-scaffold construct for 5 min. The construct was washed with distilled water and examined under phase contrast microscope and photographed.

STATISTICAL ANALYSIS

Statistical analysis was performed for MTT assay using one-way ANOVA test, with $P < 0.05$ considered as being statistically significant. Cell culture experiments were performed six times individually (n=6) and the experimental results are represented as mean values with ±standard deviations (SD).

RESULTS AND DISCUSSION

In this study, fabrication of silk fibroin–chitosan–gelatin–alginate composite scaffold in bead form was done successfully by applying foaming method without using surfactant. The size of 50 beads as determined by Image-J software (Java version) is in range of 1–3 mm with an average bead-size 2±0.5mm. The composite scaffold was characterized by ESEM, FT-IR, porosity, mechanical stability, and *in vitro* biodegradation. The biocompatibility of the composite scaffold towards skin tissue engineering was evaluated by seeding L929 fibroblasts cells over the scaffold.

Scaffold Morphology

Figure 2(a–f) showed ESEM images of the silk fibroin–chitosan–gelatin–alginate composite scaffold. The pores were spread over the entire scaffold. The ESEM images, at higher magnification markedly indicated the presence of open and interconnected pores of different sizes on the surface of the scaffold shown by an arrow marks. The pore size range of the composite scaffold was 5–230 μm (mean 92±11.8 μm). This range was higher as compared to that obtained in chitosan–gelatin–alginate scaffold fabricated in our previous study,[6] which showed the pore size range 5–106 μm. The large range of pore size obtained in this study might be due to formation of more stable foam during fabrication process thereby resulting in better pore distribution. The composite scaffold also has many smaller pores (5–15 μm) which are supposed to facilitate nutrient diffusion throughout the scaffold. In some studies, it has been revealed that smaller pores play a vital role in nutrient diffusion, cell growth, and proliferation.[33] Cross section of the scaffold was also examined as shown in Figure 2(d–f). Sectioned beads also revealed highly porous structures with interconnectivity. Thus, the 3D architecture of the scaffold possesses sufficiently porous morphology with pore-to-pore interconnections.

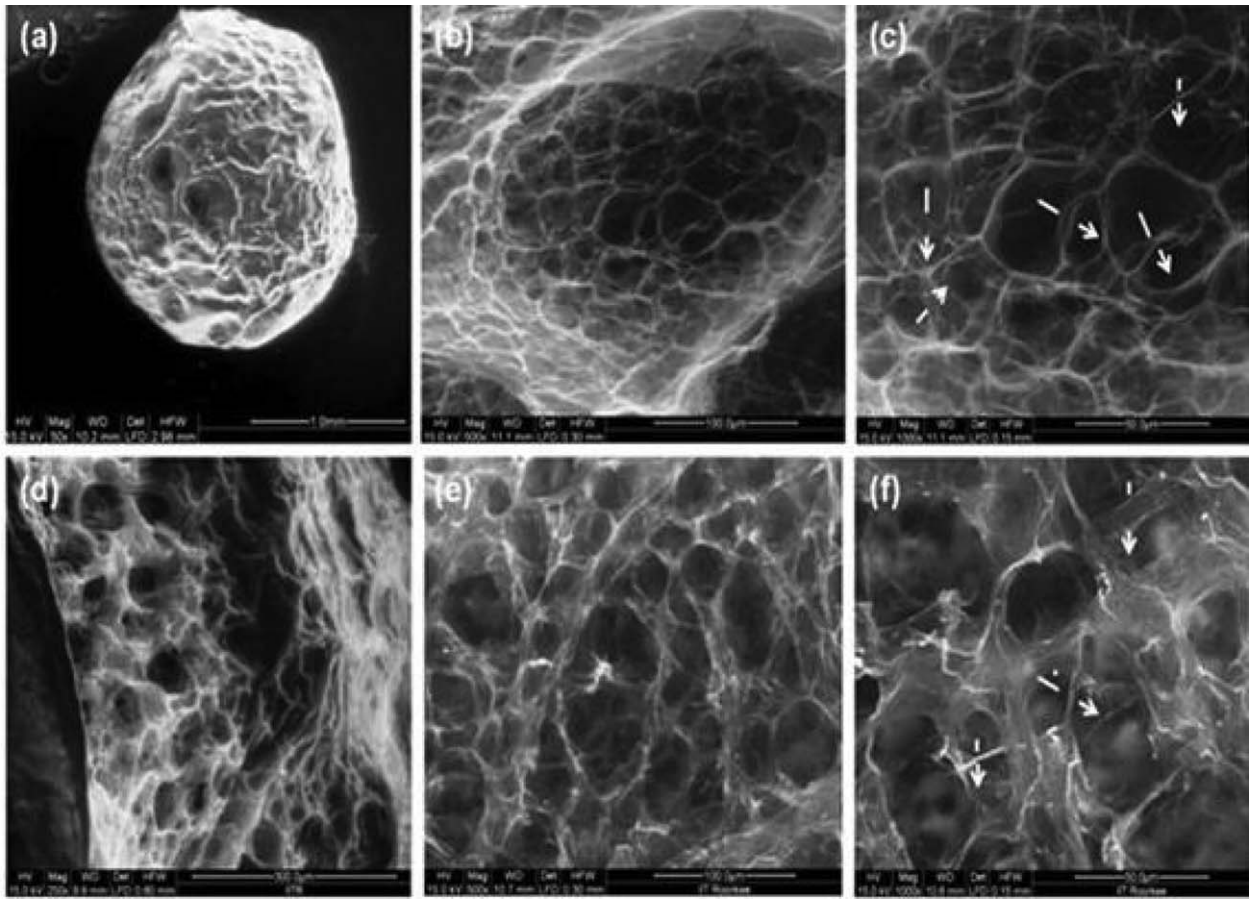

Figure 2. Scaffold morphology by ESEM analysis: (a, b, c) silk fibroin–chitosan–gelatin–alginate composite scaffold at 50×, 500×, and 1000×, respectively; (d, e, f) Cross-section of composite scaffold at 250×, 500×, and 1000×, respectively.

Fourier Transform Infrared Spectroscopy (FT-IR)

FT-IR spectra of (a) chitosan, (b) gelatin, (c) alginate, (d) Silk fibroin, and (e) composite beads were shown in Figure 3. The IR spectrum of chitosan confirms the presence of O–H and N–H stretching vibration at 3442 cm^{-1}, in which the –OH stretching vibration are overlapped by N–H stretching. The band at 1641 cm^{-1} corresponds to N–H bending vibrations of secondary amide. The C–O–C, C–O, and C–OH bending was visible at 1173 cm^{-1}. The C–H bending was seen at 1378 cm^{-1}. The band at 900 cm^{-1} corresponds to the saccharide structure of chitosan. IR spectrum of gelatin showed band at 3443 cm^{-1} due to N–H stretching of secondary amide, C=O stretching at 1639 cm^{-1}, N–H bending at 1543 cm^{-1}, and N–H out-of-plane wagging at 665 cm^{-1}. The C–N stretching bands were between 1078 cm^{-1} and 1240 cm^{-1}. The IR spectrum of alginate showed characteristic bands for its glucoronic (G) and manuronic (M) acid units at 1031 cm^{-1} and 1091 cm^{-1}, respectively. The O–H stretching band was observed at 3407 cm^{-1}. The H–C–H and O–C–H stretching vibration was seen at 1416 cm^{-1}. The $–COO^-$ stretch was visible at 1610 cm^{-1}. The bands at 886 cm^{-1} and 818 cm^{-1} indicate β-glycosidic linkages between G and M units of alginate. The IR spectrum of silk fibroin showed bands at around 1625 cm^{-1} to 1650 cm^{-1} corresponding to amide I (C=O stretching), 1524 cm^{-1} (amide II), 1235 cm^{-1} (amide III), and 665 cm^{-1} (amide V). The band located between 1625–1650 cm^{-1} can be attributed to the silk-II structure.[34–36] Silk-II is an antiparallel β-pleated sheet structure, which exists in natural silk fibroin fibers or can be produced from aqueous silk fibroin solutions treated with physical shear or organic solvents.[37]

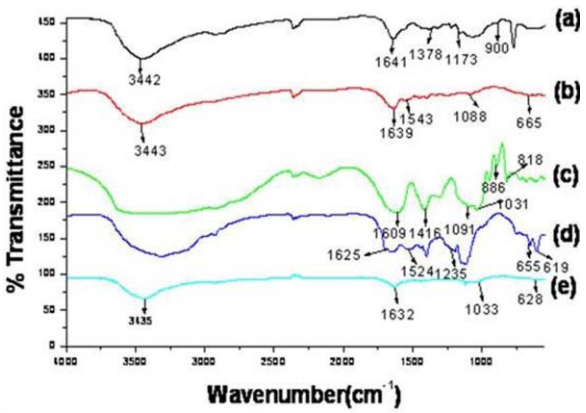

Figure 3. FT-IR spectra of (a) chitosan; (b) gelatin; (c) alginate; (d) silk fibroin; and (e) silk fibroin–chitosan–gelatin–alginate composite scaffold. [Color figure can be viewed in the online issue, which is available at wileyonlinelibrary.com.]

The IR spectrum of composite scaffold showed a very low intensity band at 1632 cm^{-1}. The band of the amino group seen in chitosan (1173 cm^{-1}) was absent in composite scaffold.

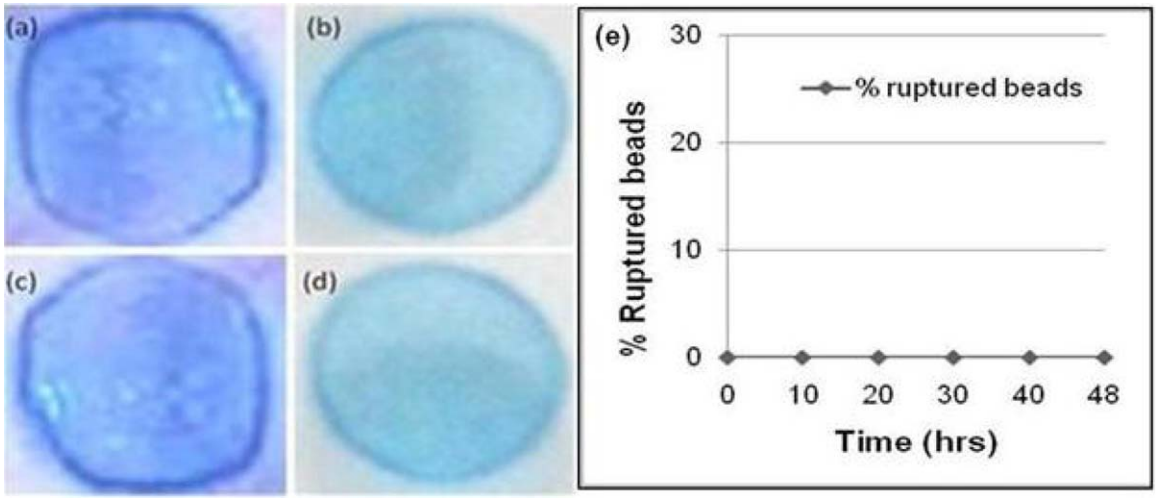

Figure 4. Silk fibroin–chitosan–gelatin–alginate composite beads (a, b) before agitation; (c, d) after 48 h agitation under physiological conditions (Magnification: 20× for all images); and (e) Percentage of ruptured beads in PBS as a function of time. [Color figure can be viewed in the online issue, which is available at wileyonlinelibrary.com.]

The amide I and amide V bands of silk fibroin at 1625 cm^{-1} and 655 cm^{-1} has been shifted to 1632 cm^{-1} and 628 cm^{-1}, respectively in the composite scaffold. Shifting of the bands in FT-IR of composite scaffold revealed that there exist some chemical interactions between the polymers used for scaffold fabrication.

Porosity

Scaffolds needs to have high porosity as it plays a critical role in cellular functionality.[38] Porosity of silk fibroin–chitosan–gelatin–alginate scaffold beads was about 88% (mean porosity 86.8%±1.90), which is sufficiently enough to facilitate cell seeding, cell diffusion, and nutrient diffusion throughout the whole structure of the scaffold. However, this porosity is less compared to porosity of chitosan–gelatin–alginate scaffold without silk fibroin fabricated in previous studies[6] in which the porosity was reported to be about 93% (mean porosity 91.8±1.90%). The decrease in porosity can be attributed to the ionic interaction between protonated amines of chitosan with carboxylate moieties on silk fibroin.[22] Nazarov and coworkers has reported that the porosity varies in range of 87–97% in silk fibroin scaffold.[39] Another study showed that porosity of approximately 86% is better for the proliferation and migration of human foreskin fibroblast cells over silk based scaffold.[40]

Contrary to this result, She and coworkers obtained a porosity of above 95% in silk fibroin and chitosan based scaffolds.[41] This may be due to different methods they used for scaffold fabrication.

Evaluation of Mechanical Stability

A short-term mechanical stability assay was carried out by exposing the silk fibroin–chitosan–gelatin–alginate composite scaffold beads to both agitation and osmotic swelling pressure in PBS solution under physiological conditions.

By this preliminary study, it was demonstrated that by the end of 48 h agitation, the beads showed only slight deformation in shape that is expected as the bead is a soft hydrogel structure (Figure 4). Nevertheless, none of the beads showed any rupturing, which indicates good mechanical stability of the scaffold

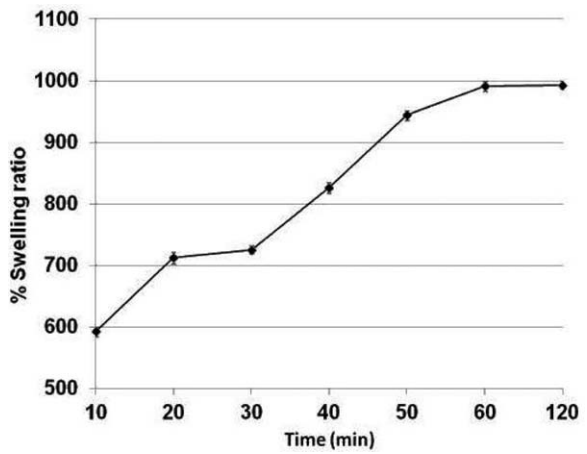

Figure 5. Swelling ratio (%) of silk fibroin–chitosan–gelatin–alginate composite scaffold.

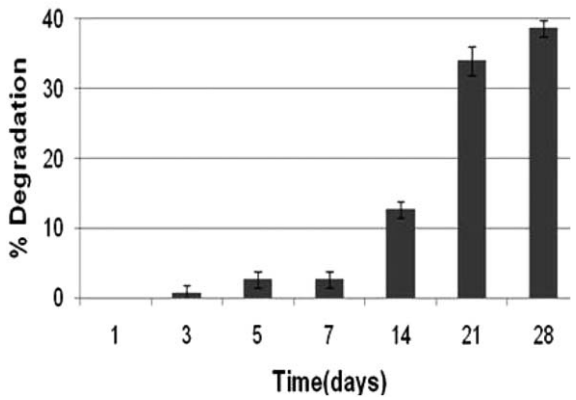

Figure 6. Percentage degradation of silk fibroin–chitosan–gelatin–alginate composite scaffold in lysozyme–PBS solution.

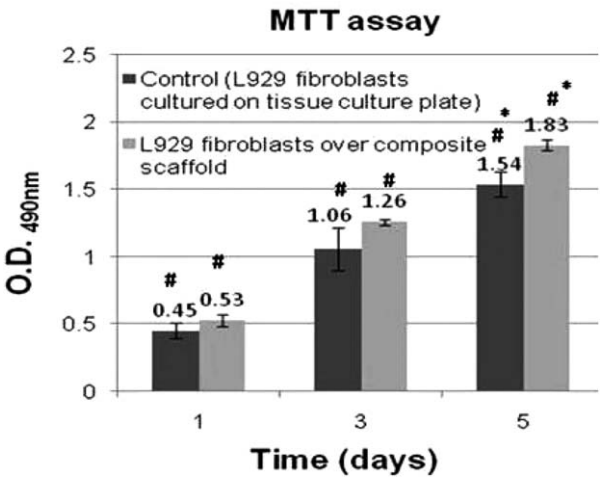

Figure 7. Viability of L929 mouse fibroblast cells on silk fibroin–chitosan–gelatin–alginate scaffold up to 5 days. Here, O.D. is directly proportional to cell viability. (*) stands for significant difference between control and scaffold on the same culture day ($P < 0.05$); (#) represents significant difference between the same samples on different culture days ($P < 0.05$).

under physiological conditions. Contrary to this, chitosan–gelatin–alginate fabricated in previous study,[6] showed deformation and slight rupturing after 10 h of agitation, which goes on increasing with agitation time. Figure 4(e) showed no rupturing of beads atleast upto 48 h of agitation. The mechanical stability of the scaffold beads was perhaps due to the presence of silk fibroin in the scaffold that is known to produce mechanically stronger scaffolds.[21,42,43] Silk fibroin is known to interact with chitosan via ionic interaction between carboxylate moieties on silk fibroin and protonated amines on chitosan.[22] This interaction could lead to formation of interpenetrating network of good mechanical properties.[17,18,22] This ionic interaction might be the basis of formation of more stable and compact scaffold structure.

It is to be mentioned here that no specific experiment has been performed for mechanical testing. However, it is noteworthy that the reported values of compression modulus for chitosan, gelatin, alginate, and silk fibroin indicated that if these polymers are combined together, then we can expect the scaffold with high mechanical strength. The reported values of these polymers in different studies are as follows: For chitosan: 3.26 ± 2.5 MPa;[44] Gelatin: 1.591 ± 0.210 kPa,[45] which can be increased by crosslinking treatments; Alginate: 20–30 kPa;[46] Silk fibroin: 3330 +/– 500 KPa;[47] 3.74 MPa (i.e., 3740 kPa);[41] and for silk fibroin/chitosan composite scaffolds ~6.53 MPa. It is reported that on increasing the concentration of either chitosan or silk fibroin, better mechanical strength can be obtained.[41] Therefore, it is expected that if we combine all these polymer then we can get a scaffold with even improved and higher mechanical properties.

Swelling Ratio

Figure 5 shows that the swelling ratio of silk fibroin–chitosan–gelatin–alginate scaffold beads, after immersion in PBS for 10 min, is about 600% and, thereafter, swelling ratio increases with time. After 60 min, no further swelling of beads (negligible swelling effects) was observed, which indicates that the equilibrium point of swelling was reached, and the equilibrium swelling ratio is approximately 992%. This result showed the hydrophilic nature of the composite scaffold. The hydrophilicity of the scaffold serve as one of the crucial factor in evaluating biomaterials for tissue engineering as it is essential for the absorption of the body fluid, which consist of water mainly, and for transfer of cell nutrient and metabolites. However, the swelling observed in silk fibroin–chitosan–gelatin–alginate scaffold was less than the swelling observed in chitosan–gelatin–alginate scaffold fabricated without silk fibroin in which equilibrium point was reached at about 1030% in 60 min.[6] The decrease in swelling ratio can be attributed to the presence of silk fibroin in the scaffold that has created a more compact and

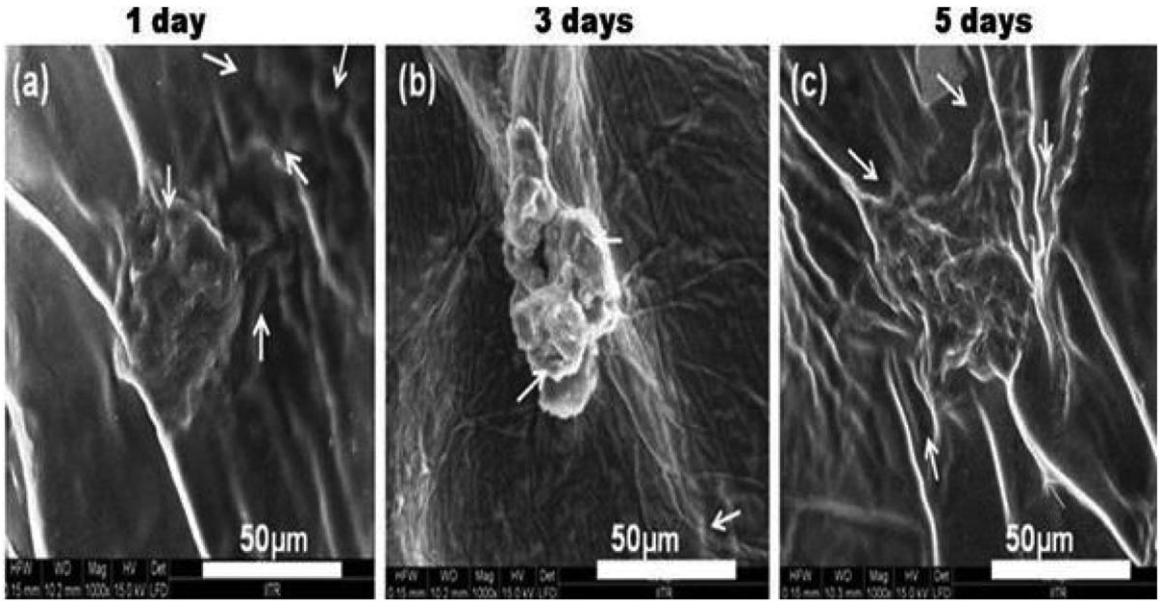

Figure 8. ESEM images of L929 fibroblast cells cultured on silk fibroin–chitosan–gelatin–alginate composite scaffold (Magnification: 1000×). White arrows indicate the cells over the scaffold.

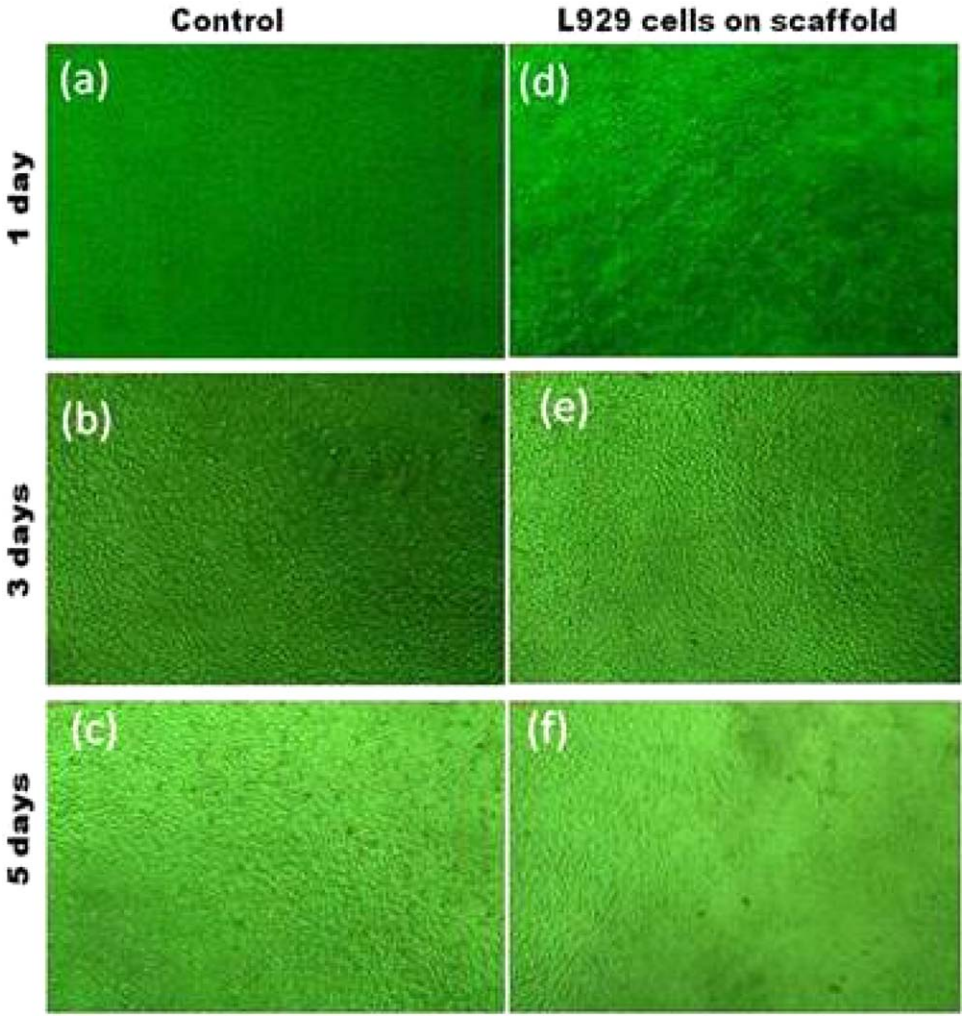

Figure 9. Phase contrast microscopy of L929 cells-scaffold constructs. It is to be emphasized here, that some of the cells are less focused in d, e, f because they are on the 3D scaffold bead which have an uneven surface as compared to the cells present in the control wells (Magnification: 10× for all images). [Color figure can be viewed in the online issue, which is available at wileyonlinelibrary.com.]

stable scaffold structure after crosslinking between the constituents of the scaffold. This structural compactness and stability of the scaffold might be responsible for hindering the mobility and relaxation of the macromolecular polymeric chains, thereby, lowering the swelling ratio, due to restriction in water mobility through the scaffold.[43,48] Thus, the decrease in the swelling ratio can be correlated with the scaffold compact structure formed after crosslinking.[43,48] Overall, the scaffold is hydrophilic which indicates that the composite scaffold can be applied potentially for skin tissue engineering applications.

In Vitro Enzymatic Biodegradation

The degradation of silk fibroin–chitosan–gelatin–alginate composite scaffold was studied in PBS–lysozyme solution (Figure 6). It was found no degradation at day 1 and from day 3 the scaffold starts degrading. The degradation of the composite scaffold after 28 days was 38% (Figure 6). However, chitosan–gelatin–alginate scaffold fabricated in previous studies[6] showed approximately 70% degradability in 21 days only under physiological condition. This indicates that the addition of silk fibroin has reduced the degradation of scaffold to a great extent. The reduced degradation rate of the scaffold might be beneficial,[49,50] as it can provide sufficient time for the formation of neo-tissue and ECM during tissue regeneration. The decrease in degradation rate of the silk fibroin based scaffolds has also been well reported in the literature.[49,50]

CELL BEHAVIOR ON THE SCAFFOLD

Cell Viability, Proliferation, and Attachment Over the Scaffold

MTT assay was performed for 1, 3, and 5 days to evaluate the cell viability and proliferation of L929 fibroblast cells over silk fibroin–chitosan–gelatin–alginate composite scaffold as shown in Figure 7. Cells seeded on a tissue culture plate without scaffold, was taken as a control. The absorbance values i.e., O.D. was measured for the cell-seeded scaffolds. The results showed successive increase in absorbance values of L929 cell-scaffold construct compared with the control. This indicated that the cells were not only viable but also showed proliferative tendency over the scaffold. The addition of silk fibroin in the scaffold increases the viability of L929 cells compared to the chitosan–gelatin–alginate composite scaffold without silk fibroin fabricated in earlier study.[6]

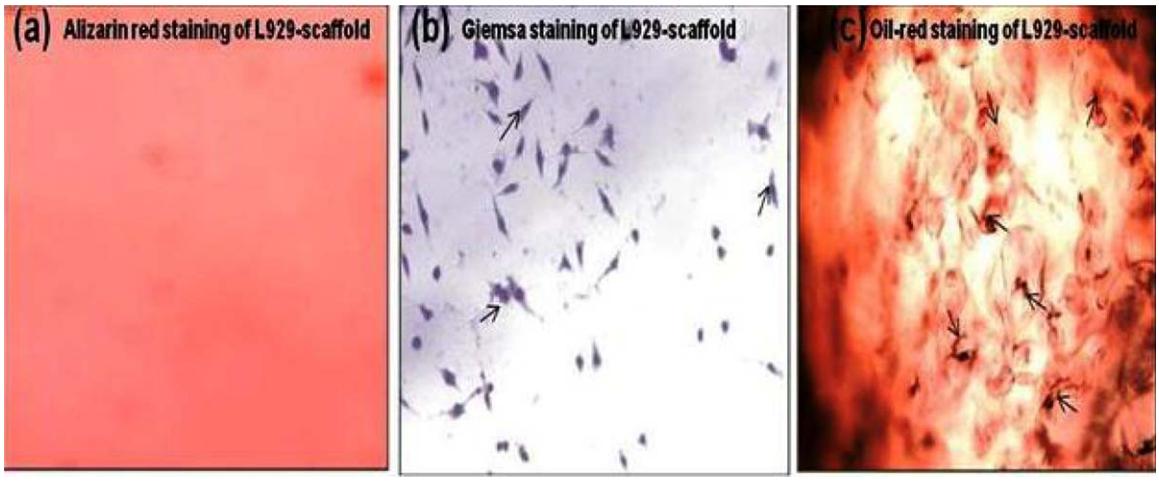

Figure 10. Alizarin, Giemsa, and Oil Red staining of L929 fibroblasts (a, b, c) after 5 days incubation with silk fibroin–chitosan–gelatin–alginate composite scaffold (Magnification: 20×). Black arrows indicate the cells present over the scaffold. [Color figure can be viewed in the online issue, which is available at wileyonlinelibrary.com.]

The better proliferation of the L929 cells over silk fibroin–chitosan–gelatin–alginate composite scaffold is believed due to higher attachment of the cells over the scaffold surface and the higher attachment might be due to the presence of silk fibroin in the scaffold. The silk fibroin can interact with the chitosan present in the scaffold to form interpenetrating network[22] and this interaction can provide sufficient chemical cues to the cells for their attachment and proliferation over the scaffold. Thus, the L929 mouse fibroblast cells showed good viability and proliferation over silk fibroin–chitosan–gelatin–alginate composite scaffold. This result is in agreement with the previous study of silk fibroin based scaffolds,[22] and confirms good cytocompatibility of L929 fibroblasts over the scaffold.

Figure 8(a–c) shows that the L929 fibroblast cells adhered to the scaffold surface after 1, 3, and 5 days. After one day, it was observed that, L929 cells adhere to the scaffold surface with rounded morphology. After three days, the L929 cells showed spreading tendency over the scaffold and after five days, the fibroblasts had taken a typical spindle-shaped morphology and exhibited cytoplasmic projections strongly attached to the scaffold, which is an indication of cell activation and proliferation [Figure 8(a–c)]. A similar type of morphology of L929 cells on chitosan-based scaffold was reported in previous studies.[51] Thus, ESEM analysis showed that the composite scaffold facilitated the L929 cells to adhere, grow, and proliferate. This result was also corroborated with MTT assay, which confirmed the potential of silk fibroin–chitosan–gelatin–alginate composite scaffold towards skin tissue engineering.

Figure 9 showed the phase contrast microscopy of the cell-scaffold construct that reveal the presence of viable and healthy cells, which increased in density with incubation time. This result supports the MTT assay result and also indicates increase in cell viability and proliferation with incubation time.

Overall, the result of cell viability and attachment study showed that silk fibroin–chitosan–gelatin–alginate composite scaffold provided a well-suited environment for the adherence and proliferation of L929 fibroblast cells. Thus, silk fibroin–chitosan–gelatin–alginate composite scaffold can be a good candidate for skin regeneration.

Histological Staining of Cell-Scaffold Construct

The L929 fibroblast cells were stained with Giemsa, Alizarin Red, and Oil Red stains to study their morphology over the scaffold. The results are shown in Figure 10. Giemsa staining showed fibroblastic morphology of L929 cells, having elongated cells with nuclei and faint cytoplasm as expected and also observed by other scientist.[52] These cells are positive for Oil Red stain indicating the presence of lipid droplet. This result was well correlated with the study by Florence and coworkers who showed that human fibroblasts from dermis and retroocular muscle were able to accumulate Oil Red positive droplets spontaneously without any differentiation induction when fibroblasts were cultured on glass slides.[53] A similar result were obtained by spontaneous lipid droplet accumulation found in L929 and NIH/3T3 mouse fibroblast cell lines when the cells were cultured on glass slides.[54] It was further shown that L929 cells stained negative for Alizarin Red staining indicating that they maintained their dermal fibroblastic phenotype and were not differentiated into bone cells or any other cell types in presence of composite scaffold (Figure 10).

The results of histological staining further supports the growth and viability of L929 mouse skin fibroblasts over the scaffold, thereby proving the great prospective of this scaffold for skin tissue engineering applications. These observations suggest that the composite scaffold matrix does not have any impact on the phenotype of L929 fibroblast cells. L929 cells maintained their fibroblastic phenotype even in the presence of the scaffold. This reveals the biocompatible nature of the silk fibroin–chitosan–gelatin–alginate composite scaffold for skin tissue engineering applications.

CONCLUSIONS

First time in the world, natural composite scaffold comprising of chitosan, gelatin, alginate, and silk fibroin was fabricated successfully by foaming method—one of the simplest and cheapest

methods of scaffold fabrication. All the polymers used for scaffold fabrication was of natural origin and these polymer combination mimic the extracellular matrix of the body to a good extent. The inclusion of silk has provided an additional advantage by imparting mechanical stability to the scaffold, and created more suitable environment for the growth and proliferation of the L929 fibroblast cells. The prolonged degradation time provided by addition of silk fibroin in the composite scaffold might be a feature that offers sufficient time for the formation of neo-tissue and ECM. All the characteristics of the scaffold as explained indicate the high potentiality of the scaffold for skin regeneration.

STATEMENT DESCRIBING THE CONTRIBUTION OF EVERY LISTED AUTHOR

This manuscript was thoroughly reviewed by all the listed authors. The corresponding author Dr. N.C. Mishra is the Principal Investigator of this work, under whose supervision Chhavi Sharma, a research scholar and the then PhD student in the lab of Dr. N.C. Mishra, carried out all the works. Dr. A.K. Dinda and Dr. Potdar provided the cell culture facilities in their labs for doing biocompatibility assays and advised for the manuscript preparation for the portion of biocompatibility assays.

ACKNOWLEDGMENTS

The authors are grateful to the Council of Scientific and Industrial Research (Grant No. 27(0222)/10/EM R-II dated May 31, 2010), as well as Ministry of Human Resources and Development (MHRD), India, for funding this research work. We are thankful to Management of Jaslok Hospital and Research Centre, Mumbai and Mr. Sachin Ramdas Chaugule, Research Assistant, Department of Molecular Medicine and Biology, for his co-operation in carrying out the biocompatibility experiments.

REFERENCES

1. Zilberman, M.; Elsner, J. J. *J. Control. Release* **2008**, *130*, 202.
2. Groeber, F.; Holeiter, M.; Hampel, M.; Hinderer, S.; Schenke-Layland, K. *Adv. Drug Delivery Rev.* **2011**, *63*, 352.
3. Gupta, S.; Sharma, C.; Dinda, A. K.; Ray, A. K.; Mishra, N. C. *J. Biomim. Biomater. Tissue Eng.* **2011**, *12*, 59.
4. Gupta, S. K.; Dinda, A. K.; Potdar, P. D.; Mishra, N. C. *Mater. Sci. Eng. C* **2013**, http://dx.doi.org/10.1016/j.msec.2013.05.045.
5. Sharma, C.; Gautam, S.; Dinda, A. K.; Mishra, N. C. *Adv. Mat. Lett.* **2011**, *2*, 90.
6. Sharma, C.; Dinda, A. K.; Mishra, N. C. *J. Appl. Polym. Sci.* **2013**, *127*, 3228.
7. Mondal, D.; Tiwari, A. *Biomed. Mater. Diagnostic Devices* **2012**, 561.
8. Zhang, C.; Subramanian, H.; Grailer, J. J.; Tiwari, A.; Pilla, S.; Steeber, D. A.; Gong, S. *Polym. Adv. Technol.* **2009**, *20*, 742.
9. Peter, M.; Ganesh, N.; Selvautmurugan, N.; Nair, S. V.; Furuike, T.; Tamura, H.; Jayakumar, R. *Carbohydr. Polym.* **2010**, *80*, 687.
10. Sachlos, E.; Czernuszka, J. T. *Eur. Cell Mater.* **2003**, *5*, 39.
11. Eiselt, P.; Rachel, J. Y.; Latvala, K.; Shea, L. D.; Mooney, D. *J. Biomaterials* **2000**, *21*, 1921.
12. Sharma, C.; Dinda, A. K.; Mishra, N. C. *J. Biomater. Tissue Eng.* **2012**, *2*, 133.
13. Mourya, V. K.; Inamdar, N. N.; Tiwari, A. *Adv. Mat. Lett.* **2010**, *1*, 11.
14. Terada, D.; Kobayashi, H.; Zhang, K.; Tiwari, A.; Yoshikawa, C.; Hanagata, N. *Sci. Technol. Adv. Mater.* **2012**, *13*, 015003.
15. Prabhakar, S.; Bajpai, J.; Bajpai, A. K.; Tiwari, A. *Polym. Bull.* **2014**, *71*, 977.
16. Ramya, R.; Venkatesan, J.; Kim, S. K.; Sudha, P. N. *J. Biomater. Tissue Eng.* **2012**, *2*, 100.
17. Drury, J. L.; Dennis, R. G.; Mooney, D. J. *Biomaterials* **2004**, *25*, 3187.
18. Kweon, H.; Ha, H.; Um. I.; Park, Y. H. *J Appl. Polym. Sci.* **2001**, *80*, 928.
19. Kang, G. D.; Lee, K. H.; Ki, C. S.; Nahm, J. H.; Park, Y. H. *Macromol. Res.* **2004**, *12*, 534.
20. Liu, H.; Xu, W.; Zou, H.; Ke, G.; LiW, O. C. *Mater. Lett.* **2008**, *62*, 1949.
21. Omenetto, F. G.; Kaplan, D. L. *Science* **2010**, *329*, 528.
22. Bhardwaj, N.; Kundu, S. C. *Carbohydr. Polym.* **2011**, *85*, 325.
23. Jin, H. J.; Chen, J.; Karageorgiou, V.; Altman, G. H.; Kaplan, D. L. *Biomaterials* **2004**, *25*, 1039.
24. Sah, M. K.; Pramanik, K. *Int. J. Environ. Sci. Dev.* **2010**, *1*, 404.
25. Lowry, O. H.; Rosebrough, N. J.; Farr, A. L.; Randall, R. J. *J. Biol. Chem.* **1951**,*193*, 265.
26. Lin, K. H.; Mishra, N.; Liu, Y. L.; Wang, C. C. U.S. Patent No. US20110091972, **2011**.
27. Karageorgiou, V.; Kaplan, D. *Biomaterials* **2005**, *26*, 5474.
28. Orive, G.; Hernandez, R. M.; Gascon, A. R.; Igartua, M.; Rojas, A.; Pedraz, J. L. *Int. J. Pharm.* **2003**, *259*, 57.
29. Tangsadthakun, C.; Kanokpanont, S.; Sanchavanchavanalit, N.; Banaprasert, T.; Damrongsakkul, S. *J. Met. Mater. Miner.* **2006**, *16*, 37.
30. Sharma, Y.; Tiwari, A.; Hattori, S.; Terada, D.; Sharma, A. K.; Ramalingam, M.; Kobayashi, H. *Int. J. Biol. Macromol.* **2012**, *51*, 627.
31. Tiwari, A.; Sharma, Y.; Hattori, S.; Terada, D.; Sharma, A. K.; Turner, A. P. F.; Kobayashi, H. *Biopolymers* **2013**, *99*, 334.
32. Huang, J. W.; Chen, W. J.; Liao, S. K.; Yang, C. Y.; Lin, S. S.; Wu, C. C. *Chang Gung Med. J.* **2006**, *29*, 363.
33. Lan Levengood, S. K.; Polak, S. J.; Wheeler, M. B.; Maki, A. J.; Clark, S. G.; Jamison, R. D.; Wagoner Johnson, A. *J. Biomaterials* **2010**, *31*, 3552.
34. Chen, X.; Shao, Z. Z.; Knight, D. P.; Vollrath, F. *Proteins* **2007**, *68*, 223.
35. Jin, H. J.; Park, J.; Karageorgiou, V.; Kim, U. J.; Valluzzi, R.; Cebe, P.; Kaplan, D. L. *Adv. Funct. Mater.* **2005**, *15*, 1241.

36. Lu, Q.; Hu, X.; Wang, X. Q.; Kluge, J.; Lu, S. Z.; Cebe, P.; Kaplan, D. L. *Acta Biomater.* **2010**, *6*, 1380.

37. Jin, H.; Kaplan, D. L. *Nature* **2003**, *424*, 1057.

38. Khan, F.; Ahmad, S. R. In Biomimetics: Advancing Nanobiomaterials and Tissue Engineering; Ramalingam, M.; Wang, X.; Chen, G.; Ma, P.; Cui, FZ., Eds.; Scrivener Publishing LLC, **2013**; Chapter 5, p 91.

39. Nazarov, R.; Jin, H. J.; Kaplan, D. L. *Biomacromol.* **2004**, *5*, 718.

40. Loh, Q. L.; Choong, C. *Tissue Eng. B Rev.* **2013**, *19*, 485.

41. She, Z.; Jin, C.; Huang, Z.; Zhang, B.; Feng, Q.; Xu, *J. Mater. Sci. Mater. Med.* **2008**, *19*, 3545.

42. Mandal, B. B.; Kundu, S. C. *Macromol. Biosci.* **2008**, *8*, 807.

43. Bajpai, A. K.; Giri, A. *Carbohydr. Polym.* **2003**, *53*, 271.

44. Chesnutt, B. M.; Viano, A. M.; Yuan, Y.; Yang, Y.; Guda, T.; Appleford, M. R.; Ong, J. L.; Haggard, W. O.; Bumgardner, J. D. *J. Biomed. Mater. Res. A* **2009**, *88*, 491.

45. Byju, A. G.; Kulkarni, A. Mechanics of Gelatin and Elastin Based Hydrogels as Tissue Engineered Constructs; In ICF13, **2013**.

46. Kuo, C. K.; Ma, P. X. *J. Biomed. Mater. Res. A* **2008**, *84*, 899.

47. Kim, U. J.; Park, J.; Kim, H. J.; Wada, M.; Kaplan, D. L. *Biomater.* **2005**, *26*, 2775.

48. Vasconcelos, A.; Gomes, A. C.; Cavaco-Paulo, A. *Acta Biomater.* **2012**, *8*, 3049.

49. Horan, R. L.; Antle, K.; Collette, A. L.; Wang, Y.; Huang, J.; Moreau, J. E.; Volloch, V.; Kaplan, D. L.; Altman, G. H. *Biomaterials* **2005**, *26*, 3385.

50. Mauney, J. R.; Nguyen, T.; Gillen, K.; Kirker-Head, C.; Gimble, J. M.; Kaplan, D. L. *Biomaterials* **2007**, *28*, 5280.

51. Mano, J. F.; Silva, G. A.; Azevedo, H. S.; Malafaya, P. B.; Sousa, R. A.; Silva, S. S.; Boesel, L. F.; Oliveira, J. M.; Santos, T. C.; Marques, A. P.; Neves, N. M.; Reis, R. L. J. R. *Soc. Inter.* **2007**, *4*, 999.

52. Harris David, M.; Inbal Hazan-Haley,; Kevin, C.; Carlos Bueso-Ramos, Jie, L.; Zhiming, L.; Ping, L.; Ravoori, M.; Abruzzo, L.; Han, L.; Singh, S.; Sun, M.; Kundra, V.; Kurzrock, R.; Estrov, Z. *PLoS One* **2011**, *6*, e21250.

53. Jeney, F.; Dombi, E. B.; Oravecz, K.; Szabo, J.; Zs-Nag, I. *Acta Histochem.* **2000**, *102*, 381.

54. Sorisky, A.; Pardasani, D.; Gagnon, A.; Smith, T. J. *J. Clin. Endocrinol. Metab.* **1996**, *81*, 3428.